Earth and Planetary Science Letters 449 (2016) 89–95

Contents lists available at ScienceDirect

Earth and Planetary Science Letters

www.elsevier.com/locate/epsl

Lithospheric architecture and deformation of NE Tibet: New insights on the interplay of regional tectonic processes

Xiaoyu Guo [a,*], Rui Gao [a], Sanzhong Li [b,c], Xiao Xu [a], Xingfu Huang [a], Haiyan Wang [a], Wenhui Li [a,*], Shujuan Zhao [b,c], Xiyao Li [b,c]

[a] Key Laboratory of Earthprobe and Geodynamics, MLR, Institute of Geology, Chinese Academy of Geological Sciences, Beijing, China
[b] College of Marine Geosciences, Ocean University of China, Qingdao, China
[c] Laboratory for Marine Geology, Qingdao National Laboratory for Marine Science and Technology, Qingdao, China

ARTICLE INFO

Article history:
Received 18 February 2016
Received in revised form 26 May 2016
Accepted 27 May 2016
Available online 6 June 2016
Editor: P. Shearer

Keywords:
deep seismic reflection image
residual gravity
NE Tibet
lithospheric architecture
deformation pattern

ABSTRACT

GPS measurements indicate rapid lateral extrusion of the NE Tibetan Plateau, which causes active NE-directed crustal shortening and has initiated oblique shearing along the margins of NE Tibet. However, the Tibetan highlands terminate around 103°E longitude and topographic relief disappears to the northeast. The exact reasons for this drop in elevation remain obscure due to widespread Tertiary sediments and Quaternary loess, which obscure details of the lithospheric structure. This study describes a new 310 km-long deep seismic reflection line striking NE-SW across the interior of NE Tibet. Integrating its data with a previously described 165 km-long deep seismic profile of the Tibet–Ordos transition zone together, these datasets provide a complete picture of the crustal architecture of the north-easternmost Tibetan Plateau. Gravity anomaly and previous geological evidence also help constrain complex deformation pattern in the region. Interpretations of these patterns indicate the importance of the large-scale sinistral Haiyuan fault zone and inherited vertical variation in mechanical properties of the lithosphere in the overall tectonic evolution of the NE Tibetan Plateau. The overall crustal architecture obtained in this study provides spatial context for the neotectonic evolution of NE Tibet and helps constrain the interplay of geologic and geodynamic processes affecting NE Tibet and adjacent regions.

1. Introduction

The Himalayan orogeny elevated the Tibetan Plateau to over 5000 m, an elevation that is compensated by crustal thickness reaching 65–75 km in certain areas (e.g. Searle et al., 2011; Zhang et al., 2011). As mean elevations have risen, increasing pressure gradients have triggered outward growth of the plateau (Meyer et al., 1998; Yuan et al., 2013) along regional strike-slip faults (Tapponnier et al., 2001).

The NE Tibetan Plateau is bounded by the Haiyuan–Liupan Shan fault system to the north and northeast and by the West Qinling sinistral fault zone to the south (Fig. 1). Contractional deformation of the plateau began in the early Tertiary time (Dayem et al., 2009; Clark et al., 2010; Zhang et al., 2010; Wang et al., 2013). Current GPS measurements indicate continuous lateral extrusion and crustal shortening of north-easternmost Tibet at a rate of ~13 mm/yr (inset in Fig. 1) (Chen et al., 2000; Gan et al., 2007). This rate is only slightly less than that across the Himalayas (Gan et al., 2007). However, the Tibetan highlands terminate around 103°E (Fig. 1). The NE corner of the plateau averages 2000 to 2500 m in elevation, resting 1500 m beneath the Qilian Shan to the west and ~2000 m lower than the southern rim of Tibet (Fig. 1). Failing to consider the influence of continuous northeastward plateau growth from 8–15 Ma activity on the Haiyuan–Liupan Shan fault, some studies have mistaken the Yumu Shan (99°30′E–100°E, 39°N–39°20′N) for the northeastern edge of the Tibetan Plateau (e.g. Tapponnier et al., 1990, 2001). Previous studies have also focused primarily on tectonic extrusion of the NE Tibetan Plateau in areas west of 103°E (Tapponnier et al., 1990, 2001; Gaudemer et al., 1995; Meyer et al., 1998). The expression of extrusion in the north-easternmost area of the Tibetan Plateau has received less attention probably due to Tertiary sediments and Quaternary loess, which obscure structural clues. Indeed, the interior of the north-easternmost Tibetan Plateau shows no signs of significant deformation. Factors contributing to the lack of topographic relief in the NE corner of the plateau have thus eluded study and interpretation. Previous teleseismic receiver function studies have deduced a predominantly felsic crustal composition for this area based on its low relative Poisson's ra-

* Corresponding authors.
E-mail addresses: xguo0515@126.com (X. Guo), dereklee1984@126.com (W. Li).

http://dx.doi.org/10.1016/j.epsl.2016.05.045

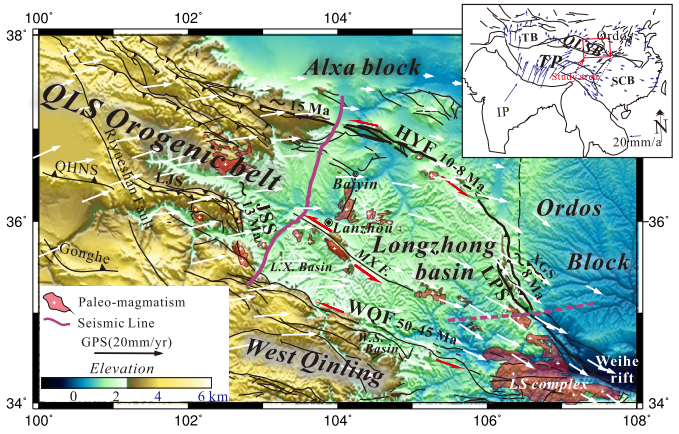

Fig. 1. Topographic map of the north-easternmost Tibetan Plateau, showing the location of the 310 km-long seismic reflection profile (purple line) and the location of the 165 km-long seismic reflection profile (dashed purple line). GPS data (white arrows) were obtained from Gan et al. (2007). The inset shows regional GPS measurements and research area (red box). Locations of plutons were included from the 1:2.5 Million Geological Map of China. TB: Tarim basin; TP: Tibetan Plateau; SCB: South China Block; IP: Indian Plate; QLSB: Qilian Shan orogenic belt; QHNS: Qinghai Nan Shan; LJS: Laji Shan; JSS: Jishi Shan; MX.F.: Maxian Shan fault; WQF: West Qinling fault; HYF: Haiyuan fault; LPS: Liupan Shan; XGS: Xiaoguan Shan; L.X.: Linxia; W.S.: Wushan; LS: Longshan.

tios (Liu et al., 2006; Pan and Niu, 2011; Zhang et al., 2013; Wang et al., 2014). The absence of mafic lower crust beneath the NE corner of the plateau adds additional contextual complexity to the area's interpretation.

To further understand this enigmatic piece of the regional puzzle, we conducted a deep seismic reflection experiment in NE Tibet. The line ran nearly N-S, in an orientation as close to orthogonal to the Haiyuan and West Qinling fault systems as terrain would allow (Fig. 1). Integrating the new seismic data with regional gravity anomalies and information from previous studies, we imaged crustal architecture beneath the NE corner of Tibet and interpret its interactions with adjacent regions.

2. Tectonic settings

An important tectonic element of the northern Tibetan Plateau, the Qilian orogenic belt developed from a protracted series of tectonic events beginning in the early Paleozoic (Xiao et al., 2009; Xu et al., 2010). The Qilian Shan represents a patchwork of units and structures amalgamated through subduction-related processes and a subsequent suturing of a Mariana-type intra-oceanic arc (North Qilian) and a Japan-type arc (Central Qilian) (Xiao et al., 2009). Evidence of this amalgamation process consists of island arc assemblages, accretionary prisms, ophiolites and high to ultrahigh-pressure metamorphic rocks exposed at the surface (Xiao et al., 2009; Yang et al., 2015). With the exception of occasional exposures of Baiyin arc and Lanzhou arc plutons, as well as the Longshan complex in the southeastern corner of NE Tibet (Fig. 1), original orogenic features have disappeared from easterly areas of the Qilian Shan. The Linxia and Longzhong basins cover areas previously occupied by mountain belts (Fig. 1).

The Cenozoic India–Eurasia collision caused diachronous deformation along the outer margins of the NE Tibetan Plateau. The event initially appears at the southern margin of NE Tibet as displacement along the WNW-trending West Qinling fault zone at 45–50 Ma (Clark et al., 2010; Duvall et al., 2011). During this time, the West Qinling fault zone experienced rapid cooling and exhumation (Clark et al., 2010; Duvall et al., 2011). Accelerated growth of the WNW-trending Laji Shan to the west (Fig. 1) commenced at 22 Ma (Lease et al., 2011). Together with the Qilian orogenic belt, these WNW-trending fault zones accommodated NNE-directed plate convergence. A directional shift in plateau growth from NNE to ENE began around ~15 Ma (Lease et al., 2011). This tectonic reorganization initiated the Jishi Shan at ~13 Ma (Lease et al., 2011). It also caused initial shearing of the Haiyuan fault zone at ~15 Ma along its western/central fault segment and at 8–10 Ma along its eastern segment (Duvall et al., 2013). Stratigraphic interpretation, apatite fission track analysis, and thermal history models suggest an intensification of deformation in the NE corner of Tibet in the later Miocene (Lin et al., 2011). The widespread oblique thrusting in the Qilian region contemporaneously merged eastward to be more localized along the Haiyuan–Liupan Shan fault system as a result (Fig. 1) (Gaudemer et al., 1995). Rapid uplift of the Liupan Shan fold-thrust belt along the northeastern margin of the Tibetan Plateau was recorded at ~8 Ma (Zheng et al., 2006). The Haiyuan–Liupan Shan fault system and West Qinling fault zone apparently merge in westerly areas of the Weihe graben system, which probably terminates east at the Tanlu fault (Zhang et al., 1995). During the Quaternary, the Ordos block to the east of the Tibetan Plateau rotated 31.5° ± 11.4° in a counterclockwise direction about a pole of rotation at its southwestern margin relative to the Qinling orogenic belt (Li et al., 2001). This process caused the southeastward opening of the Weihe graben (Zhang et al., 1995).

In the interior of the north-easternmost Tibetan Plateau, the Linxia basin is separated from most of the Longzhong basin by the sinistral Maxian Shan fault zone (Fig. 1). The Maxian Shan fault zone is interpreted to have caused the 1125 A.D. *Ms* 7.0 Lanzhou Earthquake and remains active (Yuan et al., 2002, 2008). Both the basins (i.e. the Longzhong and the Linxia) consist of Cenozoic sedimentary rocks that cover expansive areas of the NE corner of the Tibetan Plateau between the sinistral Haiyuan–Liupan Shan fault system and the left lateral West Qinling fault zone (Fig. 1). The Longzhong basin began to subside and accumulate sediment since Early Tertiary (Song et al., 2001; Horton et al., 2004). It also experienced renewed deformation later in the Paleogene (Wang et al., 2013), as the Linxia basin to the southwest of the Longzhong basin underwent a ~20° clockwise rotation (Fang et al., 2003; Dupont-Nivet et al., 2004, 2008). The Wushan basin to the north of the West Qinling fault zone (Fig. 1) began to accumulate sediments at ~16 Ma and its formation relates to tectonic deformation along the West Qinling fault zone (Wang et al., 2012).

Contractional events in NE Tibet increased its crustal thickness to 48–54 km (Zhang et al., 2013). In contrast, sedimentary basins formed from inelastic extensional deformation evidenced by surface normal faults. Previous stratigraphic studies provide additional evidence that Tertiary sedimentation in the Longzhong basin occurred in association with transtensional deformation of NE Tibet (Wang et al., 2013). Regional observations and the kinematic interpretations of basin-bounding structures indicate that the contractional response to the Himalayan orogeny has been localized in the NE corner of the Tibetan Plateau during the early Cenozoic (Dayem et al., 2009; Clark et al., 2010; Zhang et al., 2010).

3. Geophysical data

3.1. Long deep seismic reflection data

The deep seismic-reflection image described below traversed a 310 km length through a central area where is critical to understanding deformational structures affecting the NE corner of Tibet (Fig. 1). This profile runs from the Haiyuan fault in the north, through the Maxian Shan fault to the West Qinling fault in the south (Fig. 1). Gao et al. (2013) previously described northerly areas of the seismic image. This paper describes the complete set of seismic reflection data running north to south across the northeastern corner of Tibet. Data collection and processing steps fol-

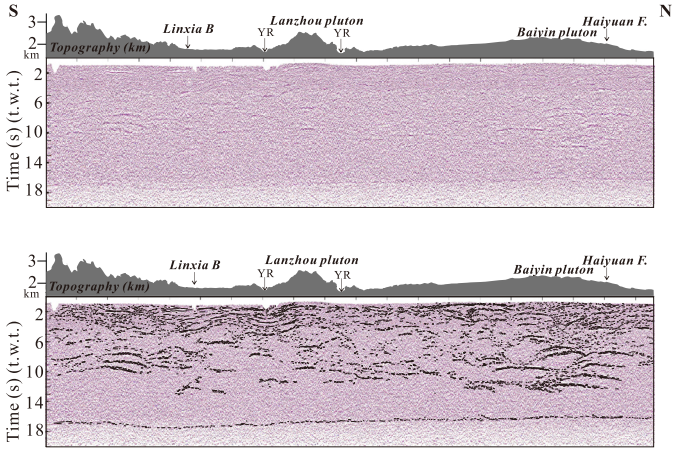

Fig. 2. A: Uninterpreted deep seismic reflection profile (no vertical exaggeration) extending from the Haiyuan fault zone, across the Maxian Shan fault zone to the West Qinling orogen (see location in Fig. 1). B: Simplified composite line drawing based on high-amplitude reflected signals in the seismic section. YR: Yellow River.

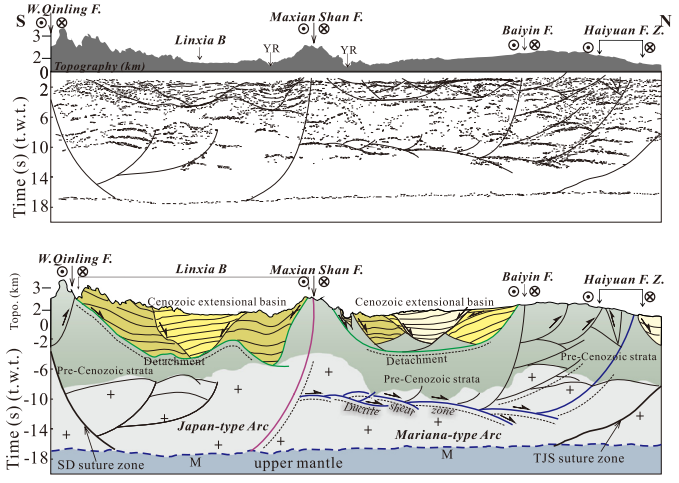

Fig. 3. A: Basic structural interpretation of the seismic profile. B: Interpretation integrating reflection patterns, previous petrologic studies and surface features. YR: Yellow River; SD: Shangdan; TJS: Tianjing Shan.

lowed that described by Gao et al. (2013). This methodology has become more or less standard among seismic reflection studies of deep lithospheric structure (e.g. Wang et al., 2011; Gao et al., 2013; Guo et al., 2013, 2015). The resulting image recorded subsurface features at depths of up to 20 s two-way time (t.w.t.) and imaged considerable complexity in the subsurface crustal structure of the NE Tibetan Plateau (Fig. 2a).

We first extracted high-amplitude signals from the reflection profile (Fig. 2b) and proceeded with a simplified composite line drawing (Fig. 3a). This step revealed highly complex crustal-scale structure which included reflections associated with extension in the uppermost crust at depths between 0 and 5 s (t.w.t) and reflections related to paleo-compression along both edges of the seismic transect at depths corresponding to 5–10 s (t.w.t.). The lower crust exhibited relatively few reflective features. The stratigraphic interpretation integrated seismic features (reflectors) with regional geologic constraints (Fig. 3b), revealing a significant vertical variations in mechanical properties of the crust.

The crustal-scale reflections divide regionally into two domains separated by a band of southwest dipping reflections that extend from the lower crust well up into the upper crust and eventually to the surface (Figs. 2a and 3b). Reflections connects with surface expressions of the left-lateral Maxian Shan fault zone (Fig. 1), indicating this structure's role in separating two distinct crustal domains: the Central Qilian to the south and the North Qilian to the north. It is noteworthy that previous wide-angle seismic studies (Zhang et al., 2013) and receiver function studies (Ye et al., 2015) also detected lateral variation in velocity structure on both sides of the Maxian Shan fault zone. Previous geochemical and petrologic studies (Xiao et al., 2009; Yang et al., 2015) further support the interpretation that the Maxian Shan fault zone represents a tectonic boundary that separates the Japan-type central Qilian arc to the south from the Mariana-type North Qilian arc to the north (Xiao et al., 2009) (Fig. 3b). In other words, the basement of NE Tibet, i.e. easterly areas of the Qilian Shan, likely consists of island arc or archipelago material rather than a stable cratonic crystalline basement.

The uppermost part of the entire seismic transect includes a series of normal faults that create small half-grabens appearing as uniform patterns of reflectivity (Figs. 2a and 3b). These normal faults are truncated at their base by two regular reflectors on each side of the Maxian Shan fault zone (2–5 s, t.w.t.). We interpret these structures as two basal detachment faults accommodating tectonic extrusion of the upper crust. Analysis of field data and regional geologic context indicates that the overall dip in reflection patterns follows regional extensional patterns that makes jogs (i.e. the Linxia basin to the south of the Maxian Shan fault zone and the majority of Longzhong basin to the north) (Wang et al., 2013) (Fig. 1). As indicated by the map view shown in Fig. 1, this geometry requires pull apart motion within the uppermost crustal wedge in order to accommodate the regional stress field. In addition to the prominent detachment structure that bounds extension-related normal faults at 2–5 s (t.w.t.), we identified an additional set of subhorizontal reflections vividly apparent to the north of the Maxian Shan fault zone at mid-crustal depths of 10 s (t.w.t.) (Figs. 2a and 3b). These features mark the boundary between the overlying crust, which exhibits complex reflection patterns, and its base, which is relatively seismically transparent. We interpreted these anomalously linear reflectors as representing a major ductile shear zone that was caught on an island arc fragment. A corresponding low velocity layer observed in both wide-angle seismic data (Zhang et al., 2013) and receiver function data (Ye et al., 2015) support this interpretation. The Maxian Shan fault zone truncates the ductile shear zone to the south, while the northernmost areas of the seismic transect show it connects to the southwest-dipping crustal-scale reflections that coincide with the Haiyuan fault zone (Figs. 2a and 3b). The Haiyuan fault zone dips to the southwest at angles of 20–30° and extends to depths greater than 12 s (t.w.t.), all the way into the upper parts of the lower crust. Geomorphologic and deep structural studies have detected sinistral shearing along the Haiyuan fault zone (e.g. Zhang et al., 1991; Burchfiel et al., 1991; Gaudemer et al., 1995; Meyer et al., 1998). Areas to the south of the Maxian Shan fault zone do not show evidence of ductile shear. The juxtaposition of extensional features with sinistral shear features, which connect to a ductile shear zone at depth, suggests that the northern segment of the seismic profile records a crustal wedge extruding to the east.

A number of reflections that dip in convex-up orientations are present within the mid-crust beneath the southernmost and northernmost edges of the seismic image (6–14 s, t.w.t.) (Figs. 2a and 3b). They formed near respective block suture zones of the Shangdan and Tianjing Shan suture zones (Fig. 1) and thus probably relate to syn-orogenic deformation during Caledonian amalgamation of the eastern Qilian Shan with both the West Qinling orogen and Alxa block.

Moho reflections indicate a thickened area at the base of the lower crust, which deepens southward from around 16 s (t.w.t) at the North Qilian to 18 s (t.w.t.) south of the Central Qilian (Fig. 2). Variation in this feature translates to crustal thicknesses ranging

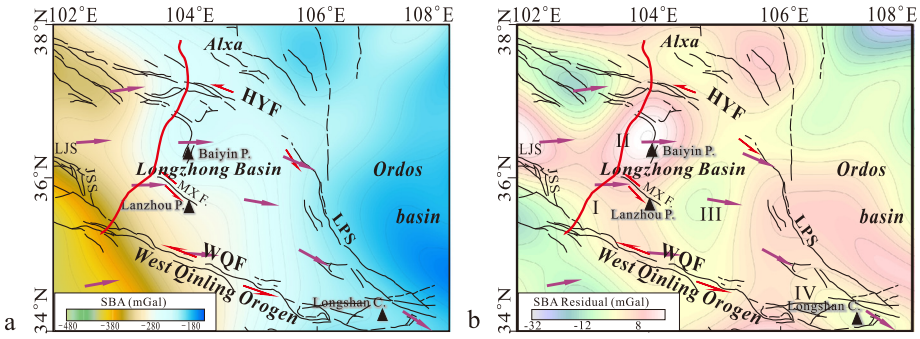

Fig. 4. A: Simple Bouguer anomaly map of the study area with a contour interval of 10 mGal. B: Residual anomaly calculated from the simple Bouguer anomaly. Black lines represent faults and purple arrows from GPS measurements (Gan et al., 2007) indicate direction of crustal extrusion. Filled triangle represents location of volcanic pluton. HYF: Haiyuan fault. LPS: Liupan Shan. WQF: West Qinling fault. MXF.: Maxian Shan fault. LJS: Laji Shan. JSS: Jishi Shan.

from 48 km in the north to 54 km to the south, assuming an average velocity of 6 km/s (e.g. Liu et al., 2006; Pan and Niu, 2011; Zhang et al., 2013; Wang et al., 2014). The Moho is laterally continuous across the seismic transect with the exception of an obscured region beneath the northern domain (Fig. 2). This anomalous area probably relates to an ecologized lower crust and subsequent delamination during arc–arc collision or possible accretionary orogeny during the early Paleozoic (Zhang et al., 2013).

3.2. Gravity anomalies

The 2D seismic profile does not entirely resolve events related to tectonic escape, especially those occurring beyond the profile. We therefore interpreted additional field data in the form of regional and residual gravity anomalies. This critical form of geophysical information can provide additional constraints to link the seismic structure and tectonic extrusion in a more perspective view.

The gravity data discussed in this study were obtained from the International Center for Global Earth Models (ICGEM). We used the same processing techniques described in Guo et al. (2014) and Xu et al. (2016) to obtain the regional Simple Bouguer gravity anomaly (Fig. 4a). According to regional scale analysis, variation in Moho depth exerts a strong influence. Values of the gravity anomalies decrease to the northeast, in association with the southwestward deepening of the Moho (e.g. Liu et al., 2006; Pan and Niu, 2011; Zhang et al., 2013; Wang et al., 2014) and indicating a northeastward crustal shortening. Areas around the Maxian Shan fault zone show a pronounced gravity gradient (Fig. 4a), which narrows from southeast to northwest. Given seismic constraints, this gravity gradient likely records crustal-scale effects of the Maxian Shan fault zone and more specifically the effects of variations in crustal thickness and lateral crustal density on either side of the structures.

In order to differentiate shallow and deep structural features, the residual gravity anomaly was obtained by isolating the first-degree trend surface polynomial from the regional Bouguer anomaly (Fig. 4b). This information helped divide the NE corner of Tibet into four areas based on the characteristic residual gravity expression in each, which are listed as I, II, III and IV in Fig. 4b. These residual gravity domains show good correlation with patterns in surface geology. In contrast to the regional Bouguer gravity anomaly, the residual gravity anomaly shows contrasting high and low gravity regions (Fig. 4b). Residual gravity domains I, II and IV reflect the masses of respective adjacent volcanic complexes: the Lanzhou pluton, the Baiyin pluton and the Longshan complex (Figs. 1 and 4b). The low-gravity domain III occurs in the middle of the study area and correlates with wide-spread Tertiary sediments and Quaternary loess throughout the majority of the Longzhong basin. Residual gravity domain I differs from the other three domains (Fig. 4b) and coincides with the Linxia basin. This gravity

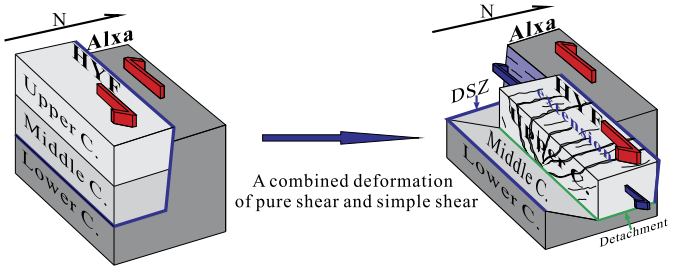

Fig. 5. Structural complexity related to vertical variation in crustal mechanical properties and sinistral shearing along the Haiyuan fault zone (not to scale). Note that the overall deformation pattern results from pure shear in the upper crust and simple shear in the middle crust. HYF: Haiyuan fault. DSZ: Ductile shear zone.

anomaly probably records the Linxia basin's response to tectonic shearing of the Maxian Shan fault zone and Jishi Shan tectonic activity to the west (Fig. 1). The other three residual gravity domains may arise from sinistral shearing of the Haiyuan fault zone. In addition, the expansive distance of individual gravity domains II and III follows a generally NE trend, while more closely spaced gravity anomalies trend subparallel to the active extrusion direction recorded by GPS measurements (Fig. 4b). Patterns in seismic structure thus indicate northeast to southeastward compression and significant southeastward horizontal mass transport occurring near the surface, as the crustal wedge of NE Tibet moves toward the West Qinling orogen. The tectonic stress field active since the Neogene reflects NE-SW compression and NW-SE extension in the NE corner of Tibet (Zhao et al., 2005). The distribution of domain IV anomalies within the south-easternmost corner of NE Tibet runs parallel to boundary faults (the Liupan Shan and West Qinling fault) (Fig. 4b), probably recording resistance from adjacent blocks during horizontal mass transport.

Overall, critical differences between regional and residual gravity anomalies indicate that the ongoing India–Eurasia collision causes a vertically incoherent response in NE Tibet due to vertical variations in crustal mechanical properties. Compression predominates in NE Tibet for example, coupled with regional-scale extension at shallow subsurface depths.

4. Discussion

4.1. Deformation pattern and regional kinematics

We developed a regional model to explain deformational patterns in NE Tibet. It synthesized the reflection profile, gravity anomalies and previous geochemical and petrologic constraints (Fig. 5). The sinistral Maxian Shan and Haiyuan fault zones form the Linxia basin and the majority of the Longzhong basin. Complex crustal deformation patterns arise from sinistral shearing along

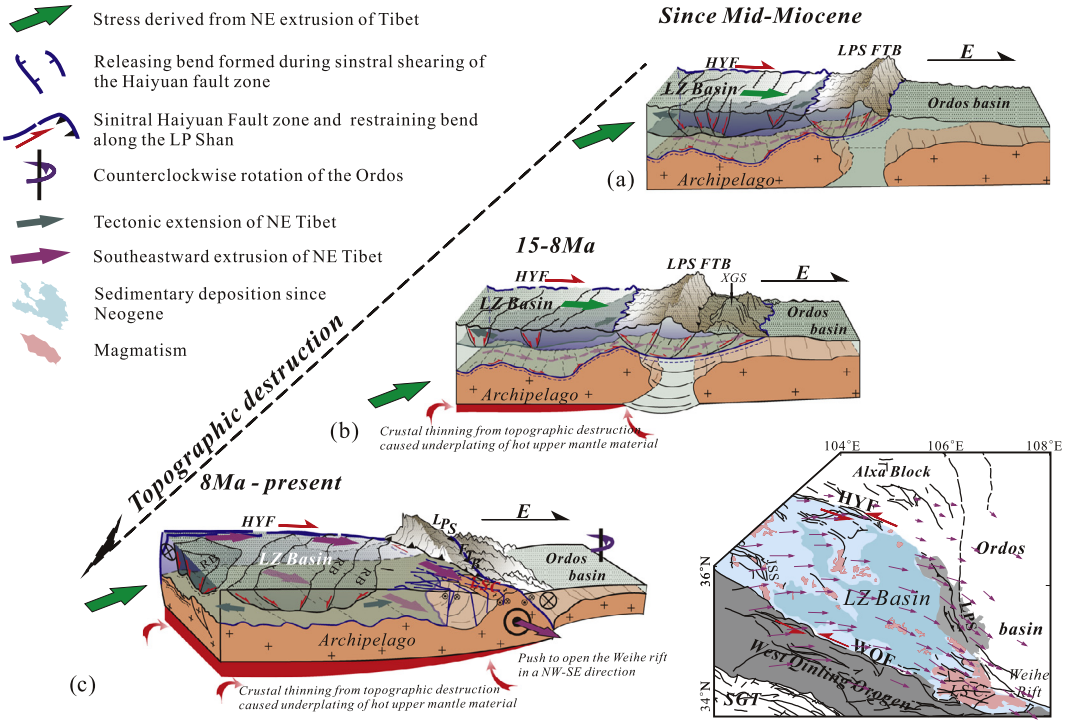

Fig. 6. Interpretive sketch (not to scale) showing the tectonic evolution of the north-easternmost Tibetan Plateau and its interactions with the adjacent Ordos block in response to far field effects of the ongoing India–Eurasia collision from middle Miocene (A) to present (C). Inset figure, edited from the 1:2.5 Million Geological Map of China, depicts the present kinematics of the NE Tibetan Plateau.

these regional scale strike-slip faults coupled with inherited vertical variation in crustal mechanical properties. Our model focused primarily on the majority of the Longzhong basin which, north of the Maxian Shan fault zone, occupies four fifths of NE Tibet (Fig. 1) and relates closely to sinistral shearing along the Haiyuan fault zone (Fig. 4b). Integration of seismic and gravity data from this study with previous geochronologic constraints suggests that the Haiyuan fault zone expressed an immediate response to middle Miocene regional plate reorganization (Lease et al., 2011). Vertical heterogeneity in crustal mechanical properties causes a complex response to sinistral shearing. Regional scale ductile shear appears as decoupled deformation between the middle and lower crust. A major detachment fault zone similarly results in decoupled deformation between the middle and upper crust. Pure shear releases bowed parts of the upper crust causing overall crustal thinning and topographic destruction. Normal faulting forms basin. In contrast, the Liupan Shan uplift within easternmost areas of the Haiyuan fault zone may help restrain bowed parts of the crust through resistance provided by the rigid basement of the Ordos block, thus creating localized steep-sided relief features. Induced simples shear in the middle crust may contribute significantly to this geometry.

4.2. Interplay of regional tectonic processes

Fig. 6 outlines the evolution of NE Tibet suggested by interpretation of the integrated datasets.

Following plate reorganization in the middle Miocene (Lease et al., 2011), the tectonic extrusion of NE Tibet shifts from northward into NE or ENE direction (Fig. 6a). As a result, a laterally contiguous crustal wedge located in the north-easternmost plateau moved toward the Ordos block. Lower crustal sections of this wedge caught on an island arc fragment causing complex deformation. The Haiyuan fault zone simultaneously began oblique sinistral motion. The crustal wedge experienced ductile shear at its base and oblique shear (Haiyuan fault zone) along its flanks. This configuration resembles a conveyor belt transporting materials eastward towards the Ordos block. To accommodate regional movement, the extensional component of deformation in the upper crust creates basins at certain points along the surface expression of the sinistral Haiyuan fault zone. Pull-apart basin form at jobs or offsets in the fault above the large-scale detachment system. The Liupan Shan uplift located along the Tibet–Ordos transition zone accommodates the contractional component of deformation caused by northeastward extrusion of Tibet and resistance from the stable Ordos block. As indicated from the 165 km-long deep seismic reflection profile (dashed purple line in Fig. 1), the ductile shear zone bounding the conveyor belt at its base subsequently extends beneath the Liupan Shan belt, causing shallow deformation within the Tibet–Ordos transition zone (Zhang et al., 1991; Guo et al., 2015). The sedimentary features separating the Mariana-type arc basement from the Ordos block in the north-easternmost Tibet are structurally inadequate to the crustal loading. Gravitational collapse of uplifted features causes eastward tectonic extrusion. Deformation progressed further eastward with continued extrusion (Fig. 6b). The contractional transition zone experience rapid uplift at ~8 Ma (Zheng et al., 2006) and expanded eastward causing the Xiaoguan Shan uplift at ~5 Ma (Zhang et al., 1991). Meanwhile, the intervening sediments beneath the Tibet–Ordos transition zone compressed against the underlying Moho layer (Wang et al., 2014; Guo et al., 2015). Horizontal orientation of strata in the Xiaoguan Shan indicates that deformation related to plateau extrusion does extend least to that feature (Guo et al., 2015). Magnetic anomalies show that the Ordos' rigid crystalline basement follows an irregular pattern along its southwestern margin (Wang et al., 2015). This pattern supports the interpretation that once eastward contraction between NE Tibet and the Ordos block reaches a critical level, deformation turns southeastward towards the Qinling orogen (Fig. 6c). Southeastward propagation of contraction simultaneously rotated the Ordos block (Li et al., 2001). The crustal wedge conveyor belt thus initiated southeastward transport of material and begins to exert stress on the Longshan complex situated at the southeastern corner of the NE Tibetan Plateau. The Longshan

complex served as a backstop, migrating forward to cause NE-SW rifting of the Weihe graben (Zhang et al., 1995).

This temporally and spatially consistent concatenation of the disparate events and features shows that NE Tibet accommodates extension through localized release of bowed upper crust along the sinistral Haiyuan fault zone. The middle crust acts as a conveyor belt, transferring stress from the east to the southeast. Together these mechanisms restore level topography and reduce overall crustal thickness. The thermal re-equilibration necessary to compensate for crustal thinning draws hot asthenosphere upward. The upwelling causes anomalously high heat flow and a relatively shallow Curie's depth (16–28 km) observed in the study area (Lei et al., 1999).

5. Conclusion

Seismic reflection data analyzed in this study provide a consistent interpretation of structural complexity in the north-easternmost corner of NE Tibet. A transect across the study area shows a series of strike-slip features accommodating tectonic escape through ductile shear in the middle crust and detachments in the upper crust. Regional- and residual gravity anomalies provide critical geophysical constraints, which highlight impediments to tectonic extrusion and thus explain deformation appearing along alternative structural pathways. The integration of seismic and gravity data helps reconcile the crustal wedge's relatively coherent lateral structure with its complex vertical structure. The active ductile shear zone above a subcrustal island arc fragment indicates unhindered transport of the crustal mass. Extension of the upper crust above large-scale detachment systems helps explain structural complexity in terms of regional models of tectonic escape. The present geomorphology of NE Tibet thus reflects the influence of lithospheric architecture and geodynamic interactions with adjacent regions.

Acknowledgements

We would give our thanks to the anonymous reviewer and Dr. Walter Mooney at USGS for their careful and thorough readings of this manuscript. Their constructive criticism and suggestions do provide us an opportunity to emphasize the main lines of evidence and add new information in support of our hypothesis. This research was supported by the National Natural Science Foundation of China (Grant No. 41430213, 41590863, 41304064, 41325009, 41190072). We thank colleagues who collected seismic data used in this study.

References

Burchfiel, B.C., Zhang, P.Z., Wang, Y.P., Zhang, W.Q., Song, F.M., Deng, Q.D., Molnar, P., Royden, L., 1991. Geology of the Haiyuan fault zone, Ningxia–Hui Autonomous region, China, and its relation to the evolution of the northeastern margin of the Tibetan Plateau. Tectonics 10, 1091–1110.

Chen, Z., Burchfiel, B.C., Liu, Y., King, R.W., Royden, L.H., Tang, W., Wang, E., Zhao, J., Zhang, X., 2000. Global positioning system measurements from eastern Tibet and their implications for India/Eurasia intercontinental deformation. J. Geophys. Res. 105, 16215–16227.

Clark, M.K., Farley, K.A., Zheng, D.W., Wang, Z.C., Duvall, A., 2010. Early Cenozoic faulting on the northern Tibetan Plateau margin from apatite (U–Th)/He ages. Earth Planet. Sci. Lett. 296, 78–88.

Dayem, K.E., Molnar, P., Clark, M.K., Houseman, G.A., 2009. Far-field lithospheric deformation in Tibet during continental collision. Tectonics 28, TC6005.

Dupont-Nivet, G., Horton, B.K., Zhou, J., Waanders, G.L., Butler, R.F., Wang, J., 2004. Paleogene clockwise tectonic rotation of the Xining–Lanzhou region, northeastern Tibetan Plateau. J. Geophys. Res. 109, B04401.

Dupont-Nivet, G., Hoorn, C., Konert, M., 2008. Tibetan uplift prior to the Eocene–Oligocene climate transition: evidence from pollen analysis of the Xining Basin. Geology 36, 987–990.

Duvall, A.R., Clark, M.K., van der Pluijm, B.A., Li, C.Y., 2011. Direct dating of Eocene reverse faulting in northeastern Tibet using Ar-dating of fault clays and low-temperature thermochronometry. Earth Planet. Sci. Lett. 304, 520–526.

Duvall, A.R., Clark, M.K., Kirby, E., Farley, K.A., Craddock, W.H., Li, C., Yuan, D.Y., 2013. Low-temperature thermochronometry along the Kunlun and Haiyuan Faults, NE Tibetan Plateau: evidence for kinematic change during late-stage orogenesis. Tectonics 32, 1190–1211.

Fang, X.M., Garzione, C., Van der Voo, R., Li, J.J., Fan, M.J., 2003. Flexural subsidence by 29 Ma on the NE edge of Tibet from the magnetostratigraphy of Linxia Basin, China. Earth Planet. Sci. Lett. 210, 545–560.

Gan, W.J., Zhang, P.Z., Shen, Z.K., Niu, Z.J., Wang, M., Wan, Y.G., Zhou, D.M., Cheng, J., 2007. Present-day crustal motion within the Tibetan Plateau inferred from GPS measurements. J. Geophys. Res. 112, B08416.

Gao, R., Wang, H., Yin, A., Dong, S.W., Kuang, Z.Y., Zuza, A.V., Li, W.H., Xiong, X.S., 2013. Tectonic development of the northeastern Tibetan Plateau as constrained by high-resolution deep seismic reflection data. Lithosphere 5, 555–574.

Gaudemer, Y., Tapponnier, P., Meyer, B., Peltzer, G., Shunming, G., Zhitai, C., Huagung, D., Cifuentes, I., 1995. Partitioning of crustal slip between linked, active faults in the eastern Qilian Shan, and evidence for a major seismic gap, the "Tianzhu gap", on the western Haiyuan fault, Gansu (China). Geophys. J. Int. 120, 599–645.

Guo, X.Y., Gao, R., Keller, R.G., Xu, X., Wang, H.Y., Li, W.H., 2013. Imaging the crustal structure beneath the eastern Tibetan Plateau and implications for the uplift of the Longmen Shan range. Earth Planet. Sci. Lett. 379, 72–80.

Guo, X.Y., Keller, R.G., Gao, R., Xu, X., Wang, H.Y., Li, W.H., 2014. Irregular western margin of the Yangtze block as a cause of variation in tectonic activity along the Longmen Shan fault zone, eastern Tibet. Int. Geol. Rev. 56, 473–480.

Guo, X.Y., Gao, R., Wang, H.Y., Li, W.H., Keller, R.G., Xu, X., Li, H.Q., Encarnacion, J., 2015. Crustal architecture beneath the Tibet–Ordos transition zone, NE Tibet, and the implications for plateau expansion. Geophys. Res. Lett. 42, 10631–10639.

Horton, B.K., Dupont-Nivet, G., Zhou, J., Waanders, G.L., Butler, R.F., Wang, J., 2004. Mesozoic–Cenozoic evolution of the Xining–Minhe and Dangchang basins, northeastern Tibetan Plateau: magnetostratigraphic and biostratigraphic results. J. Geophys. Res. 109, B04402.

Lease, R.O., Burbank, D.W., Clark, M.K., Farley, K.A., Zheng, D.W., Zhang, H.P., 2011. Middle Miocene reorganization of deformation along the northeastern Tibetan Plateau. Geology 39, 359–362.

Lei, F., Dong, Z.P., Liu, B.Q., Ma, L.H., Zhao, Y.Q., 1999. The geotemperature field in Gansu–Ningxia–Qinghai area and its relation to earthquakes. J. Gansu Sci. 11, 22–27.

Li, W.J., Lu, Y.C., Ding, G.Y., 2001. Paleomagnetic evidence from less for the relative motion between the Ordos and its adjacent blocks. Quat. Res. 21, 551–559 (in Chinese with English abstract).

Lin, X.B., Chen, H.L., Wyrwoll, K.H., Batt, G.E., Liao, L., Xiao, J., 2011. The uplift history of the Haiyuan–Liupan Shan region northeast of the present Tibetan Plateau: integrated constraint from stratigraphy and thermochronology. J. Geol. 119, 372–393.

Liu, M.J., Mooney, W.D., Li, S.L., Okaya, N., Detweiler, S., 2006. Crustal structure of the northeastern margin of the Tibetan Plateau from the Songpan–Ganzi terrane to the Ordos basin. Tectonophysics 420, 253–266.

Meyer, B., Tapponnier, P., Bourjot, L., Métivier, F., Gaudemer, Y., Peltzer, G., Guo, S.M., Chen, Z.T., 1998. Crustal thickening in Gansu–Qinghai, lithospheric mantle subduction, and oblique, strike-slip controlled growth of the Tibet Plateau. Geophys. J. Int. 135, 1–47.

Pan, S.Z., Niu, F.L., 2011. Large contrasts in crustal structure and composition between the Ordos plateau and the NE Tibetan plateau from receiver function analysis. Earth Planet. Sci. Lett. 303, 291–298.

Searle, M.P., Elliott, J.R., Phillips, R.J., Chung, S.L., 2011. Crustal–lithospheric structure and continental extrusion of Tibet. J. Geol. Soc. 168, 633–672.

Song, G.Y., Fang, X.M., Li, J.J., An, Z.S., Miao, X.D., 2001. The Late Cenozoic uplift of the Liupan Shan, China. Sci. China, Ser. D 44 (Supp.), 176–184.

Tapponnier, P., Meyer, B., Avouac, J.P., Peltzer, G., Gaudemer, Y., Guo, S.M., Xiang, H.F., Yin, K.L., Chen, Z.T., Cai, S.H., Dai, H.G., 1990. Active thrusting and folding in the Qilian Shan, and decoupling between upper crust and mantle in northeastern Tibet. Earth Planet. Sci. Lett. 97, 382–403.

Tapponnier, P., Xu, Z.Q., Roger, F., Meyer, B., Arnaud, N., Wittlinger, G., Yang, J.S., 2001. Oblique stepwise rise and growth of the Tibet Plateau. Science 294, 1671–1677.

Wang, C.S., Gao, R., Yin, A., Wang, H.Y., Zhang, Y.X., Guo, T.L., Li, Q.S., Li, Y.L., 2011. A mid-crustal strain-transfer model for continental deformation: a new perspective from high-resolution deep seismic-reflection profiling across NE Tibet. Earth Planet. Sci. Lett. 306, 279–288.

Wang, C.Y., Sandvol, E., Zhu, L., Lou, H., Yao, Z.X., Luo, X.H., 2014. Lateral variation of crustal structure in the Ordos block and surrounding regions, North China, and its tectonic implications. Earth Planet. Sci. Lett. 387, 198–211.

Wang, W.T., Kirby, E., Zhang, P.Z., Zheng, D.W., Zhang, G.L., Zhang, H.P., Zheng, W.J., Chai, C.Z., 2013. Tertiary basin evolution along the northeastern margin of the Tibetan Plateau: evidence for basin formation during Oligocene transtension. Geol. Soc. Am. Bull. 125, 377–400.

Wang, Z.C., Zhang, P.Z., Garmala, N.C., Lease, O.R., Zhang, G.L., Zheng, D.W., Hough, B., Yuan, D.Y., Li, C.Y., Liu, J.H., Wu, Q.L., 2012. Magnetostratigraphy and depositional

history of the Miocene Wushan basin on the NE Tibetan Plateau, China: implications for middle Miocene tectonics of the West Qinling fault zone. J. Asian Earth Sci. 44, 189–202.

Wang, Z.T., Zhou, H.R., Wang, X.L., Jing, X.C., 2015. Characteristics of the crystalline basement beneath the Ordos Basin: constraint from aeromagnetic data. Geosci. Front. 6, 465–475.

Xiao, W.J., Windley, B.F., Yong, Y., Yan, Z., Yuan, C., Liu, C.Z., Li, J.L., 2009. Early Paleozoic to Devonian multiple-accretionary model for the Qilian Shan, NW China. J. Asian Earth Sci. 35, 323–333.

Xu, X., Keller, R.G., Gao, R., Guo, X.Y., Zhu, X.S., 2016. Uplift of the Longmen Shan area in the eastern Tibetan Plateau: an integrated geophysical and geodynamic analysis. Int. Geol. Rev. 58, 14–31.

Xu, Y.J., Du, Y.S., Cawood, P.A., Yang, J.H., 2010. Provenance record of a foreland basin: detrital zircon U-Pb ages from Devonian strata in the North Qilian Orogenic belt, China. Tectonophysics 495, 337–347.

Yang, H., Zhang, H.F., Luo, B.J., Zhang, J., Xiong, Z.L., Guo, L., Pan, F.B., 2015. Early Paleozoic intrusive rocks from the eastern Qilian orogeny, NE Tibetan Plateau: petrogenesis and tectonic significance. Lithos 224–225, 13–31.

Ye, Z., Gao, R., Li, Q.S., Zhang, H.S., Shen, X.Z., Liu, X.Z., Gong, C., 2015. Seismic evidence for the North China plate underthrusting beneath northeastern Tibet and its implications for plateau growth. Earth Planet. Sci. Lett. 426, 109–117.

Yuan, D.Y., Liu, B.C., Cai, S.H., Liu, X.F., Wang, Y.C., 2002. Principal features of recent activity of the active northern marginal fault zone of Maxianshan mountains, Lanzhou, Gansu Province. Seismol. Geol. 24, 315–323 (in Chinese with English abstract).

Yuan, D.Y., Wang, L.M., He, W.G., Liu, B.C., Ge, W.P., Liu, X.W., Liang, M.J., Zheng, W.J., 2008. New progress of seismic active fault prospecting in Lanzhou City. Seismol. Geol. 30, 236–249 (in Chinese with English abstract).

Yuan, D.Y., et al., 2013. The growth of northeastern Tibet and its relevance to large-scale continental geodynamics: a review of recent studies. Tectonics 32, 1358–1370.

Zhang, J., Cunningham, D., Chen, H.Y., 2010. Sedimentary characteristics of Cenozoic strata in central-southern Ningxia, NW China: implications for the evolution of the NE Qinghai-Tibetan Plateau. J. Asian Earth Sci. 39, 740–759.

Zhang, P.Z., Burchfiel, B.C., Molnar, P., Zhang, W.Q., Jiao, D.C., Deng, Q.D., Wang, Y.P., Royden, L., Song, F.M., 1991. Amount and style of Late Cenozoic deformation in the Liupan Shan area, Ningxia Autonomous Region, China. Tectonics 10, 1111–1129.

Zhang, Y.Q., Vergely, P., Mercier, J., 1995. Active faulting in and along the Qinling Range (China) inferred from SPOT imagery analysis and extrusion tectonics of South China. Tectonophysics 243, 69–95.

Zhang, Z.J., Deng, Y.F., Teng, J.W., Wang, C.Y., Gao, R., Chen, Y., Fan, W.M., 2011. An overview of the crustal structure of the Tibetan Plateau after 35 years of deep seismic soundings. J. Asian Earth Sci. 40, 977–989.

Zhang, Z.J., Bai, Z.M., Klemperer, S.L., Tian, X.B., Xu, T., Chen, Y., Teng, J.W., 2013. Crustal structure across northeastern Tibet from wide-angle seismic profiling: constraints on the Caledonian Qilian Orogeny and its reactivation. Tectonophysics 606, 140–159.

Zhao, T.S., Dong, Z.P., Wang, P., 2005. Active faults and modern tectonic stress field in the region of Gansu. J. Gansu Sci. 17, 30–34 (in Chinese with English abstract).

Zheng, D.W., Zhang, P.Z., Wan, J.L., Yuan, D.Y., Li, C.Y., Yin, G.M., Zhang, G.L., Wang, Z.C., Min, W., Chen, J., 2006. Rapid exhumation at ~8 Ma on the Liupan Shan thrust fault from apatite fission-track thermochronology: implications for growth of the northeastern Tibetan Plateau margin. Earth Planet. Sci. Lett. 248, 198–208.